AD-A134 011 A POLARIZATION DIVERSITY RADAR DATA PROCESSOR(U) AIR 1/1
FORCE GEOPHYSICS LAB HANSCOM AFB MA J I METCALF ET AL.
28 APR 83 AFGL-TR-83-0111

UNCLASSIFIED F/G 17/9 NL

END
DATE FILMED
DTIC

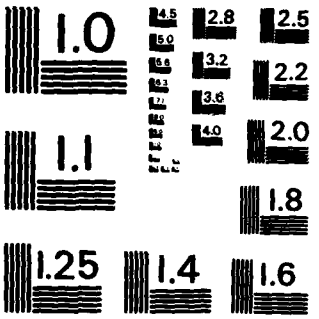

MICROCOPY RESOLUTION TEST CHART
NATIONAL BUREAU OF STANDARDS-1963-A

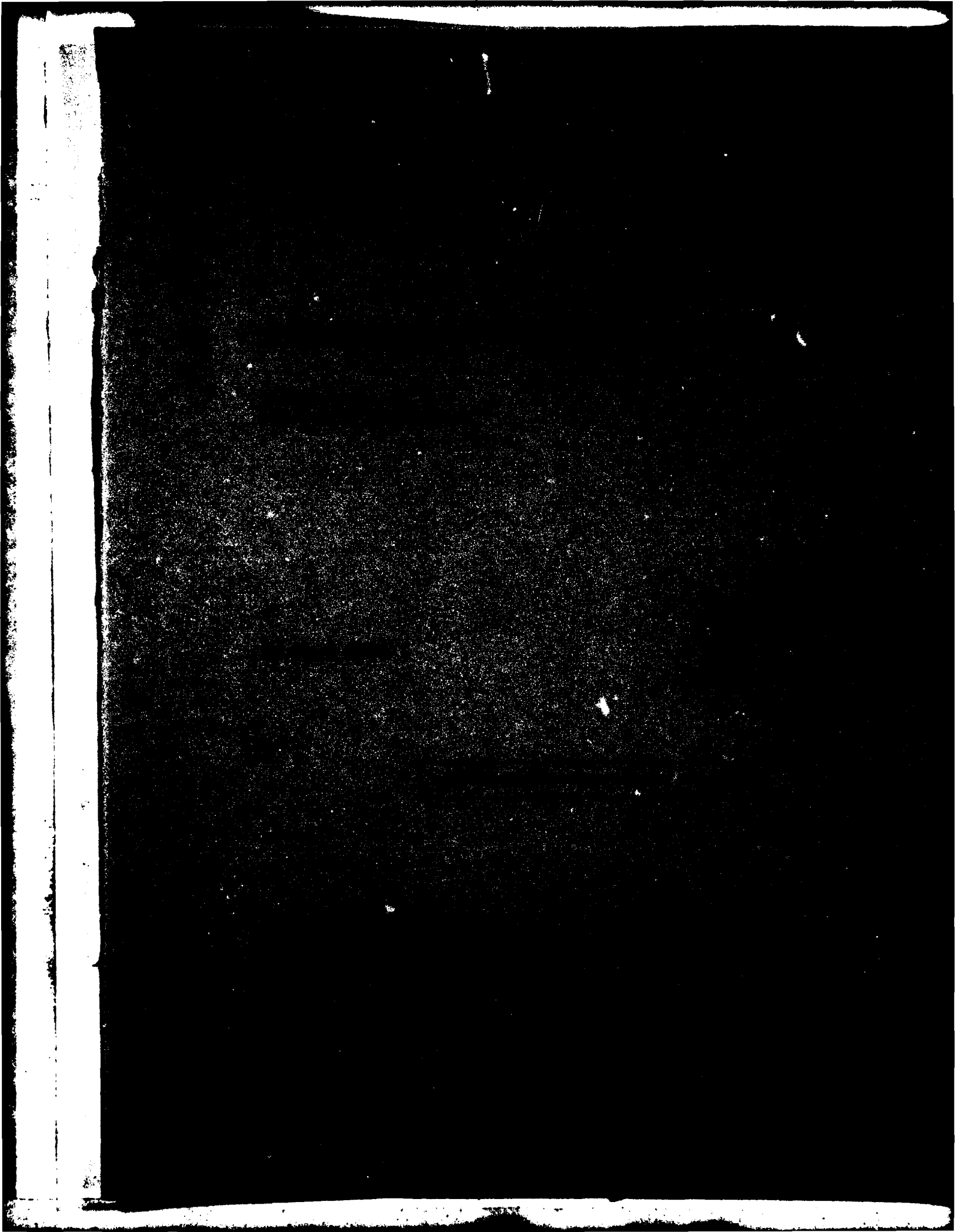

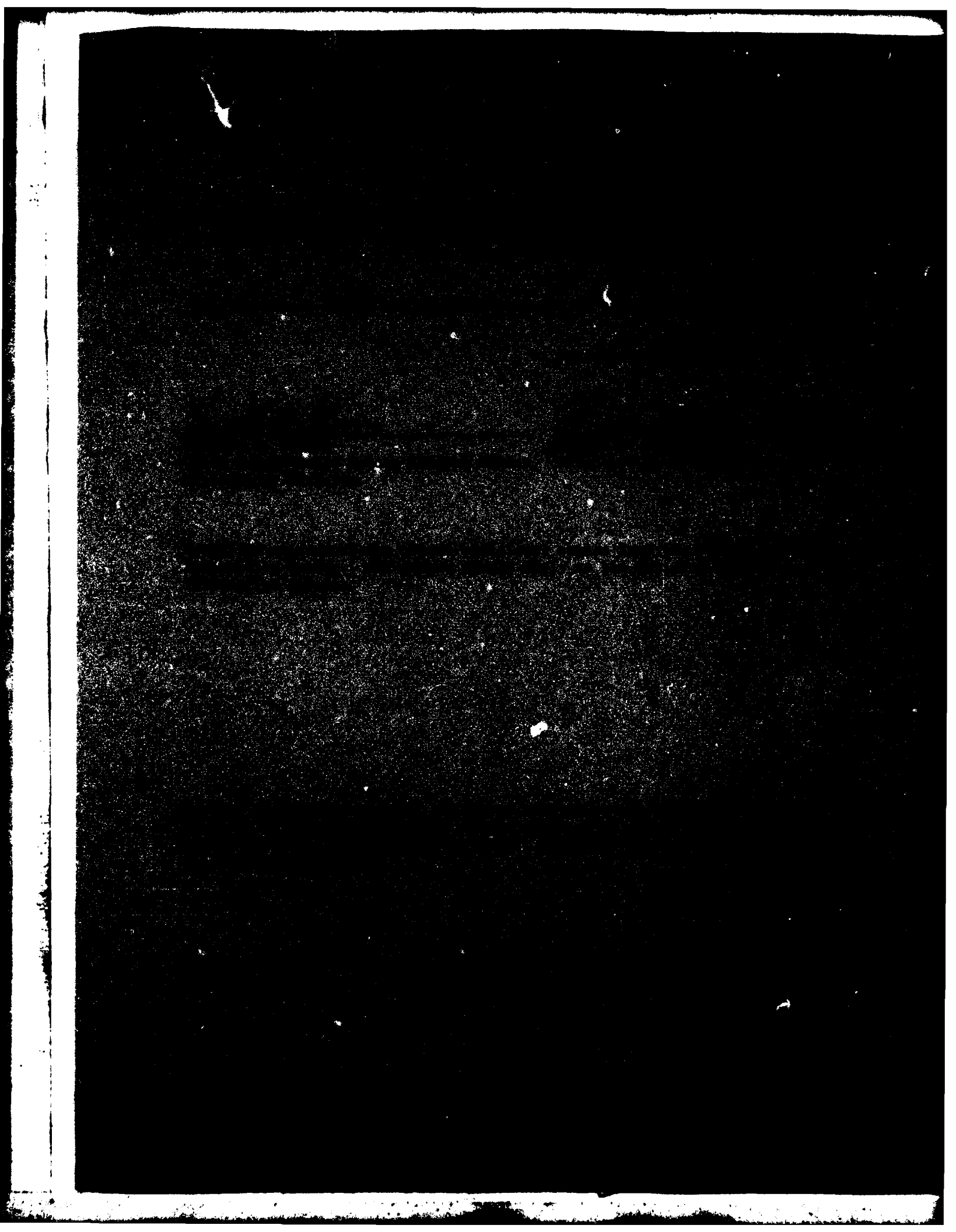

Unclassified

SECURITY CLASSIFICATION OF THIS PAGE (When Data Entered)

REPORT DOCUMENTATION PAGE	READ INSTRUCTIONS BEFORE COMPLETING FORM
1. REPORT NUMBER: AFGL-TR-83-0111	2. GOVT ACCESSION NO.: AD-A134011
3. RECIPIENT'S CATALOG NUMBER:	
4. TITLE (and Subtitle): A POLARIZATION DIVERSITY RADAR DATA PROCESSOR	5. TYPE OF REPORT & PERIOD COVERED: Scientific. Interim.
	6. PERFORMING ORG. REPORT NUMBER: IP, No. 318
7. AUTHOR(s): James I. Metcalf Graham M. Armstrong	8. CONTRACT OR GRANT NUMBER(s):
9. PERFORMING ORGANIZATION NAME AND ADDRESS: Air Force Geophysics Laboratory (LYR) Hanscom AFB Massachusetts 01731	10. PROGRAM ELEMENT, PROJECT, TASK AREA & WORK UNIT NUMBERS: 62101F 66701602
11. CONTROLLING OFFICE NAME AND ADDRESS: Air Force Geophysics Laboratory (LYR) Hanscom AFB Massachusetts 01731	12. REPORT DATE: 28 April 1983 13. NUMBER OF PAGES: 27
14. MONITORING AGENCY NAME & ADDRESS (if different from Controlling Office)	15. SECURITY CLASS. (of this report): Unclassified 15a. DECLASSIFICATION/DOWNGRADING SCHEDULE

16. DISTRIBUTION STATEMENT (of this Report)

Approved for public release; distribution unlimited.

17. DISTRIBUTION STATEMENT (of the abstract entered in Block 20, if different from Report)

18. SUPPLEMENTARY NOTES

19. KEY WORDS (Continue on reverse side if necessary and identify by block number)

Polarization-diversity weather radar
Radar data processor
Polarization switching
Signal autocovariance

20. ABSTRACT (Continue on reverse side if necessary and identify by block number)

A real time data processor has been designed for use with the AFGL 10-cm Doppler weather radar which is to be operated with alternating transmission of horizontally and vertically polarized signals. In this mode of operation the reception of backscattered signals of polarizations identical to those of the transmitted signals allows the computation of the differential reflectivity between the two polarizations in addition to the absolute reflectivity and the Doppler mean velocity and variance. The switching of transmitted polarization introduces difficulties in the estimation of the autocovariance of the received

DD FORM 1 JAN 73 1473 EDITION OF 1 NOV 65 IS OBSOLETE

Unclassified

SECURITY CLASSIFICATION OF THIS PAGE (When Data Entered)

20. (Contd)

signals, from which the Doppler velocity parameters are derived. The processor design and the allowed modes of radar operation circumvent these difficulties. This report describes the processing algorithms theoretically and presents details of the implementation of these algorithms in hardware.

Contents

Illustrations

Illustrations

Tables

A Polarization Diversity Radar Data Processor

1. INTRODUCTION

The development of a polarization diversity capability for the AFGL 10-cm Doppler weather radar[1,2] necessitates the design and construction of a new data processor to compute reflectivity, Doppler parameters, and polarization parameters in real time. The first phase of radar modification required for implementation of this capability was begun in 1982, with the long range goals of transmitting either circularly or linearly polarized signals, with rapid switching between either right and left circular or horizontal and vertical polarizations, and coherently receiving two signals of polarizations identical and orthogonal to that of the transmitted signal. The first phase involves modification of the antenna and feed system to a dual polarization configuration and the installation of a high power microwave switch. When this phase is completed, as is planned for FY 1984, the radar will have the capability of transmitting horizontally and vertically polarized signals, with rapid switching between the two polarizations, and receiving backscattered signals of polarization

(Received for publication 26 April 1983)

1. Bishop, A. W., and Armstrong, G. M. (1982) A 10-cm Dual Frequency Doppler Weather Radar, Part I: The Radar System, AFGL-TR-82-0321 (I), AD A125885.

2. Ussailis, J. S., Leiker, L. A., Goodman, R. M., IV, and Metcalf, J. I. (1982) Analysis of a Polarization Diversity Weather Radar Design, AFGL-TR-82-0234, AD A121666.

identical to that of the transmitted signals. The radar can then be used to measure the differential reflectivity as described by Seliga and Bringi.[3] This quantity, together with the absolute reflectivity derived from backscattered signals of one polarization, provides information on the shapes of particles in the backscattering medium which can be interpreted in terms of thermodynamic phase and, in rain, drop size. The measurement and interpretation of differential reflectivity has been discussed extensively in the scientific literature.

The Doppler mean velocity and variance derived from coherently received backscatter signals yield further information on the backscattering medium and provide a measure of the air flow patterns in precipitation systems. Taken together with the absolute and differential reflectivities, the Doppler velocity parameters permit the derivation of a comprehensive and detailed description of the precipitation system.

The concepts and formulations of the data processing are described in the following section. Section 3 describes the implementation of the algorithms and includes block diagrams of the processor and its components.

2. SIGNAL PROCESSING REQUIREMENTS

In this section we describe the requirements and procedures for processing Doppler velocity data, derived from the coherent receiver, and reflectivity data, derived from the logarithmic receiver. Procedures are described for the two cases of radar operation with and without polarization switching. Of particular concern for both reflectivity and Doppler velocity computations are the effects of polarization switching on the accuracy and possible bias of the computed quantities. Hence, we discuss several problems inherent in operation with switched polarization and describe the ways in which these problems are solved or circumvented in the processor design and radar operation.

2.1 Doppler Velocity Parameters

The Doppler mean velocity and variance are to be computed by means of pulse pair autocovariance techniques. In particular, the mean velocity $\bar{v}$ is to be calculated from the autocovariance at one and two pulse lage using the technique due to Rummler[4]

3. Seliga, T.A., and Bringi, V.N. (1976) Potential use of radar differential reflectivity measurements at orthogonal polarizations for measuring precipitation, J. Appl. Meteor. 15:69-76.

4. Rummler, W.D. (1968) Introduction of a New Estimator for Velocity Spectral Parameters, Tech. Memo. MM-68-4121-5, Bell Telephone Laboratories, Whippany, New Jersey.

$$\bar{v} = \frac{\lambda}{2} \cdot \frac{1}{2\pi\tau} \arg [R(\tau)] \tag{1}$$

and the technique suggested by Strauch et al.[5]

$$\bar{v} = \frac{\lambda}{2} \cdot \frac{1}{2\pi\tau} [(1/2) \arg [R(2\tau)] + n\pi] \tag{2}$$

where the value of the correction index n is determined by the arguments of $R(\tau)$ and $R(2\tau)$ as shown in Table 1.

Table 1. Value of Correction Index for Use With Autocovariance at Two-pulse Lag. Value is determined by the quadrants of the arguments of $R(\tau)$ and $R(2\tau)$. Brackets denote conditions for which derived velocity is negative

	arg [R(2τ)]			
arg [R(τ)]	$(-\pi, -\pi/2)$	$(-\pi/2, 0)$	$(0, \pi/2)$	$(\pi/2, \pi)$
$(-\pi, -\pi/2)$	[0]	1	[-1]	[-1]
$(-\pi/2, 0)$	[0]	[0]	0	[-1]
$(0, \pi/2)$	1	[0]	0	0
$(\pi/2, \pi)$	1	1	[-1]	0

Several approaches exist for the estimation of Doppler velocity variance. If the spectrum is Gaussian and the noise level is known, then an exact formula for the variance is

$$\sigma_v^2 = \frac{\lambda^2}{8\pi^2\tau^2} \ln \left| \frac{R(o) - N}{R(\tau)} \right| \tag{3}$$

where N is the average noise level. The formula developed by Rummler[4] is

$$\sigma_v^2 = \frac{\lambda^2}{8\pi^2\tau^2} \left\{ 1 - \frac{|R(\tau)|}{R(o)} (1 + SNR^{-1}) \right\} \tag{4}$$

5. Strauch, R.G., Kropfli, R.A., Sweezy, W.B., Moninger, W.R., and Lee, R.W. (1978) Improved Doppler velocity estimates by the poly-pulse-pair method. Preprints, 18th Conf. Radar Meteor., Amer. Meteor. Soc., Boston: pp. 376-380.

where SNR is the signal-to-noise ratio. The noise correction can be omitted in either of the above formulae if the signal-to-noise ratio is high. A preferred alternative is the formula proposed by Srivastava et al.[6]

$$\sigma_v^2 = \frac{\lambda^2}{24\pi^2\tau^2} \ln \left| \frac{R(\tau)}{R(2\tau)} \right| \tag{5}$$

which does not require real-time estimation of the signal-to-noise ratio. The formula is also exact for Gaussian spectra. Other estimation procedures yield better results if the Doppler spectrum is significantly non-Gaussian.[7] These are all based on the computation of the autocovariance of the received signal at several time lags. Hence, although we do not contemplate implementing these procedures, we note that they can be easily added as options in the future, since the present processor design includes the real-time computation of autocovariance at zero, one, and two-pulse lags.

The key problem in the processor design is therefore to implement optimum estimators of the autocovariance function, that is, estimators that are unbiased in both magnitude and phase. The autocovariance at zero time lag will be a sum of two categories of terms, corresponding to horizontal and vertical transmitted polarization, respectively. For complex amplitudes $A_{H(2n)}$ and $A_{V(2n+1)}$ at horizontal (H) and vertical (V) polarizations and successive times designated by 2n and 2n + 1, we have

$$\begin{aligned} \hat{R}(0) &= \frac{1}{N} \left\{ \sum_{n=0}^{\frac{N}{2}-1} A_{H(2n)} A^*_{H(2n)} + \sum_{n=0}^{\frac{N}{2}-1} A_{V(2n+1)} A^*_{V(2n+1)} \right\} \\ &= 1/2 \left\{ \hat{R}_{HH}(0) + \hat{R}_{VV}(0) \right\} \end{aligned} \tag{6}$$

where $\hat{R}_{HH}(0)$ and $\hat{R}_{VV}(0)$ are the estimates one would derive separately from signals of horizontal and vertical polarization, respectively. The expected values of these estimators are the average received powers for the two polarizations, namely

---

6. Srivastava, R. C., Jameson, A. R., and Hildebrand, P. H. (1979) Time-domain computation of mean and variance of Doppler spectra. J. Appl. Meteor. 18:189-194.

7. Passarelli, R. E., Jr., and Siggia, A. D. (1983) The autocorrelation function and Doppler spectral moments: Geometric and asymptotic interpretations. J. Clim. Appl. Meteor. 22, accepted for publication

$$E[\hat{R}_{HH}(0)] = \overline{P}_H$$

$$E[\hat{R}_{VV}(0)] = \overline{P}_V \ . \tag{7}$$

For further analysis of the autocovariance estimators one can normalize the signal amplitudes by their root-mean-square values, $(\overline{P}_H)^{1/2}$ and $(\overline{P}_V)^{1/2}$. The bias of $\hat{R}(0)$ relative to the estimate obtained from a radar operating with fixed polarization, for example, horizontal, is determined by the ratio of received power between the two polarizations, that is, the differential reflectivity. Thus:

$$\begin{aligned} E[\hat{R}(0)] &= (1/2) \left\{ E[\hat{R}_{HH}(0)] + E[\hat{R}_{VV}(0)] \right\} \\ &= (1/2) \left\{ E[\hat{R}_{HH}(0)] + \frac{\overline{P}_V}{\overline{P}_H} E[\hat{R}_{HH}(0)] \right\} \\ &= (1/2) \ (1 + \overline{P}_V/\overline{P}_H) E[\hat{R}_{HH}(0)] \ . \end{aligned} \tag{8}$$

Computation of the autocovariance at non-zero time lags requires evaluation of four categories of signal pulse pairs: (1) those having common horizontal polarization of the two transmitted pulses, (2) those having common vertical polarization, (3) those in which the first pulse is horizontally polarized and the second vertically polarized, and (4) those in which the first pulse is vertically polarized and the second horizontally polarized. We can then analyze the most general case in which any number of pulses may be transmitted during the polarization switching interval. For analysis of the autocovariance, we represent phase of the received signals explicitly, in terms of phase due to scattering and phase due to signal propagation through the radar and the atmosphere. Because the transmitted signals of orthogonal polarization follow different paths in the radar and because precipitation is typically an anisotropic propagation medium, there is a nearly constant differential phase shift (in a given measurement scenario) between received signals corresponding to orthogonally polarized transmissions. Thus we have for horizontal polarization

$$A_H = |A_H| \ e^{i(\phi_s(\tau) + \phi_H)} \tag{9}$$

and for vertical polarization

$$A_V = |A_V| \ e^{i(\phi_s(\tau) + \phi_V)} \tag{10}$$

where $\phi_s(\tau)$ is the phase due to scattering (assumed to be independent of polarization) and ϕ_H and ϕ_V are phases due to propagation in the radar and in the atmosphere at horizontal and vertical polarization, respectively. The four categories of terms available for the autocovariance estimator $\hat{R}(\tau)$ are represented by

$$A_H(0)A_H^*(\tau) = |A_H(0)|\ |A_H(\tau)|\ e^{i[\phi_s(0) - \phi_s(\tau)]} \tag{11}$$

$$A_V(0)A_V^*(\tau) = |A_V(0)|\ |A_V(\tau)|\ e^{i[\phi_s(0) - \phi_s(\tau)]} \tag{12}$$

$$A_H(0)A_V^*(\tau) = |A_H(0)|\ |A_V(\tau)|\ e^{i[(\phi_s(0) - \phi_s(\tau)) + (\phi_H - \phi_V)]} \tag{13}$$

$$A_V(0)A_H^*(\tau) = |A_V(0)|\ |A_H(\tau)|\ e^{i[(\phi_s(0) - \phi_s(\tau)) - (\phi_H - \phi_V)]} . \tag{14}$$

We assume that the phase difference $\phi_s(0) - \phi_s(\tau) = \Delta\phi(\tau)$ is a random variable independent of polarization and independent of time. The sums of the four categories of pulse pairs correspond to autocovariance estimators $\hat{R}_{HH}(\tau)$, $\hat{R}_{VV}(\tau)$, $\hat{R}_{HV}(\tau)$, and $\hat{R}_{VH}(\tau)$. By scaling the amplitudes as described above we can express the expected values of three of these estimators in terms of the expected value of $\hat{R}_{HH}(\tau)$:

$$E[\hat{R}_{VV}(\tau)] = (\overline{P}_V/\overline{P}_H)\ E[\hat{R}_{HH}(\tau)] \tag{15}$$

$$E[\hat{R}_{HV}(\tau)] = (\overline{P}_V/\overline{P}_H)^{1/2}\ E[\hat{R}_{HH}(\tau)]\ e^{i(\phi_H - \phi_V)} \tag{16}$$

$$E[\hat{R}_{VH}(\tau)] = (\overline{P}_V/\overline{P}_H)^{1/2}\ E[\hat{R}_{HH}(\tau)]\ e^{-i(\phi_H - \phi_V)} . \tag{17}$$

An analogous derivation can be developed for the computation of $\hat{R}(2\tau)$. From the results above, we can develop three estimators of $\hat{R}(\tau)$. Using equal numbers of pairs of common horizontal and vertical polarization we have

$$\hat{R}_1(\tau) = (1/2)[\hat{R}_{HH}(\tau) + \hat{R}_{VV}(\tau)] . \tag{18}$$

The expected value of this estimator

$$E[\hat{R}_1(\tau)] = (1/2)[1 + \overline{P}_V/\overline{P}_H]\ E[\hat{R}_{HH}(\tau)] \tag{19}$$

is unbiased in phase but is biased in magnitude by a function of the differential reflectivity. A second estimator involves pairs of the dissimilar polarizations, in equal numbers of those with horizontal first and those with vertical first:

$$\hat{R}_2(\tau) = (1/2)[\hat{R}_{HG}(\tau) + \hat{R}_{VH}(\tau)] . \tag{20}$$

The expected value of this estimator

$$E[\hat{R}_2(\tau)] = (\overline{P}_V/\overline{P}_H)^{1/2} E[\hat{R}_{HH}(\tau)] \cos(\phi_H - \phi_V) \tag{21}$$

is again unbiased in phase but is biased in magnitude by the square root of the power ratio and by the cosine of the differential phase shift. The differential phase shift in the system can be minimized by careful design. However, the differential phase shift in the atmosphere increases monotonically with range, and at long range through heavy precipitation it can approach 90°, at which point the expected value of $\hat{R}_2(\tau)$ is zero. This estimator could be used for mean velocity estimation, by Eq. (1), but would yield highly biased variance estimates. A third estimator can be developed by recognizing that

$$\left[\frac{E[\hat{R}_{HV}(\tau)]}{E[\hat{R}_{VH}(\tau)]}\right]^{1/2} = e^{i(\phi_H - \phi_V)} . \tag{22}$$

We use the ratio $[\hat{R}_{HV}(\tau)/\hat{R}_{VH}(\tau)]^{1/2}$ as an estimator of the phase factor $\exp[i(\phi_H - \phi_V)]$ and define the estimator as

$$\begin{aligned}\hat{R}_3(\tau) &= (1/2)\left(\hat{R}_{HV}(\tau)\left[\frac{\hat{R}_{VH}(\tau)}{\hat{R}_{HV}(\tau)}\right]^{1/2} + \hat{R}_{VH}(\tau)\left[\frac{\hat{R}_{HV}(\tau)}{\hat{R}_{VH}(\tau)}\right]^{1/2}\right) \\ &= \left(\hat{R}_{HV}(\tau)\hat{R}_{VH}(\tau)\right)^{1/2} .\end{aligned} \tag{23}$$

This estimator would be unbiased only if its expected value were equal to the product of the expected values of $[\hat{R}_{HV}(\tau)]^{1/2}$ and $[\hat{R}_{VH}(\tau)]^{1/2}$, that is, if $\hat{R}_{HV}(\tau)$ and $\hat{R}_{VH}(\tau)$ were uncorrelated. Typically, however, these estimates are highly correlated, especially if they are derived from the same sample time series. In general, for correlated random variables x and y we have

$$E(xy) = E(x)E(y) + \mathrm{Cov}(x, y) \tag{24}$$

and

$$\mathrm{Cov}(x, y) = \rho(x, y)\,[\mathrm{Var}(x)\,\mathrm{Var}(y)]^{1/2} \tag{25}$$

where Cov is the covariance, ρ the autocorrelation, and Var the variance. In the present case, $\rho \simeq 1$ so that if $x = [\hat{R}_{HV}(\tau)]^{1/2}$ and $y = [\hat{R}_{VH}(\tau)]^{1/2}$

$$E[\hat{R}_3(\tau)] \simeq E[[\hat{R}_{HV}(\tau)]^{1/2}]\, E[[\hat{R}_{VH}(\tau)]^{1/2}]$$

$$+ [\mathrm{Var}[(\hat{R}_{HV}(\tau))^{1/2}]\,\mathrm{Var}[(\hat{R}_{VH}(\tau))^{1/2}]]^{1/2} . \tag{26}$$

We have not fully analyzed the statistical properties of this estimator. The variances are approximately inversely proportional to the number of pulse pairs in the estimators $\hat{R}_{HV}(\tau)$ and $\hat{R}_{VH}(\tau)$, and can therefore be reduced by extending the length of the signal sample. In practice, the available length of the sample is limited by constraints on scanning time and spatial resolution. Hence, it is not certain that the variances can be made negligibly small or even "acceptably" small.

In summary, we find that reliable estimation of autocovariance can be accomplished only by averaging the products of signals having common polarization. The bias factor $(1 + \overline{P}_V/\overline{P}_H)$, which arises from the collective summation of pairs of horizontally polarized signals and pairs of vertically polarized signals does not affect the ratio of autocovariances at different time lags, as used in Eq. (5).

The problems inherent in the use of summations of products of signals of opposite polarizations can be alleviated in our system, as the Doppler processing and reflectivity processing are done with signals transmitted on different carrier frequencies which can be pulsed at different rates. Specifically, the carrier frequency for the coherent receiver can be pulsed at 1, 2, 3, or 4 times the pulse repetition rate of the carrier frequency for the logarithmic receiver. This feature was included in the original radar design for the purpose of resolving range and velocity ambiguities. [1] If the multiples 3 or 4 are used, then sums of products of signals of common polarization can be accumulated to estimate the autocovariance at 1 and 2 pulse time lags. Thus we will implement the estimators

$$\hat{R}_1(\tau) = (1/2)[\hat{R}_{HH}(\tau) + \hat{R}_{VV}(\tau)] \tag{27}$$

and

$$\hat{R}_1(2\tau) = (1/2)[\hat{R}_{HH}(2\tau) + \hat{R}_{VV}(2\tau)] . \tag{28}$$

The switching of transmitted polarization will signal the processor to delete from the summation those pairs of pulses spanning the change of polarization. Table 2 shows the percentage of all pairs that are usable for the autocovariance calculation, that is, that have common polarization of pulses. The processor will have the inherent capability of operating with signals of fixed polarization, since in this case all pulse pairs will be accepted.

The formulations above are based on the assumption that there are no echoes detected in the coherent receiver which are aliased in range. In practice, since the Doppler carrier frequency may be pulsed at approximately 1300 Hz with a corresponding unambiguous range of 115 km, this assumption will not generally be valid for low elevation angles. The situation is further complicated in that these range-aliased echoes may have polarization opposite to that of the radar antenna and thus be detected at a much lower power level, as determined by the polarization isolation of the antenna. Procedures for circumventing this problem are discussed in Section 4.

Table 2. Percentage of Pulse Pairs Usable for Autocovariance Calculation

(Switch interval) ÷ (Doppler Pulse Rep. Time)	Autocovariance			
	R(0)	R(τ)	R(2τ)	R(3τ)
1	100%	0%	100%	0%
2	100%	50%	0%	50%
3	100%	67%	33%	0%
4	100%	75%	50%	25%

2.2 Absolute and Differential Reflectivity

Reflectivity is customarily derived by averaging the sampled output of a logarithmic receiver, in order to achieve the widest possible dynamic range. The resulting average is approximately 2.5 dB lower than would be obtained if the power, that is, the squared signal amplitude, were averaged. For operations with fixed polarization, this procedure is adequate to yield reflectivity estimates with 90% confidence limits within ± 1 dB for typical averaging times.

A study of the statistics of differential reflectivity estimators by Bringi et al[8] showed that the estimates were consistently more accurate if the power, rather than its logarithm, is averaged. Examples of their computations are shown in Figure 1. The accuracy of the estimates of differential reflectivity depends on both the number of samples and the cross-correlation between signal samples of opposite polarizations. If successive pulses are transmitted with orthogonal polarizations then the cross-correlation is approximately equal to the autocorrelation of the received signals at one-pulse lag. The cross-correlation between successive signals of horizontal and vertical polarization is defined by

$$\rho_{HV}(\tau) = \frac{|E(A_H A_V^*)|}{[E(|A_H|^2)\, E(|A_V|^2)]^{1/2}} \tag{29}$$

where A_H and A_V are amplitudes of successive received signals of horizontal and vertical polarization. In terms of autocovariance functions it can be written as

$$\rho_{HV}(\tau) = \frac{|R_{HV}(\tau)|}{[R_{HH}(0) R_{VV}(0)]^{1/2}} \tag{30}$$

where the autocovariance function $R_{HV}(\tau)$ implies the summation of products of *signals of opposite polarization for which the horizontally polarized signal is first*, and $R_{HH}(0)$ and $R_{VV}(0)$ are the autocovariance functions computed for signals of horizontal and vertical polarizations, respectively. One must use the partial sum of pulse pairs implied in $R_{HV}(\tau)$ to avoid the bias in expected value resulting from differential phase shifts in the radar and in the atmospheric propagation medium.

The differential reflectivity is obtained most accurately from successive signal samples with opposite polarization. The receiver outputs will be converted to actual power, corrected for noise, and accumulated in two registers corresponding to the two transmitted polarizations. At the end of each averaging interval, the contents of one register are used to determine the absolute reflectivity (at horizontal polarization), and the estimate of differential reflectivity in decibels is computed from the logarithm of the ratio of the two sums. The cross-correlation of the signal samples is to be estimated from the Doppler velocity variance, computed from the coherent receiver output.

---

8. Bringi, V. N., Seliga, T. A., and Cherry, S. M. (1983) Statistical properties of the dual-polarization differential reflectivity (Z_{DR}) radar signal. IEEE Trans. Geoscience and Remote Sensing, GE-21:215-220.

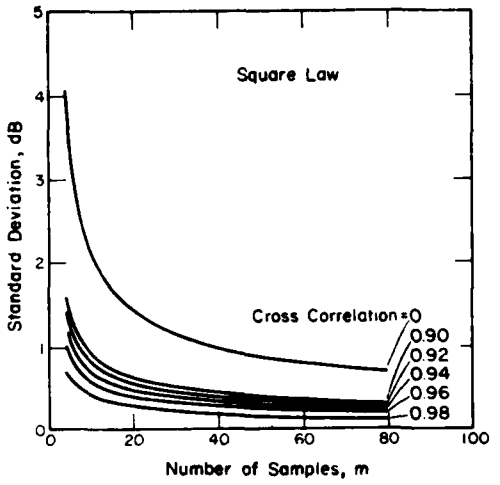

Figure 1a. Standard deviation of estimate of differential reflectivity, expressed in decibels, as a function of the number of samples of each polarization, based on averages of the squared amplitude measured at each polarization for several values of the cross-correlation coefficient between successive samples of opposite polarization. [After Bringi et al (1983), Reference 8 © IEEE]

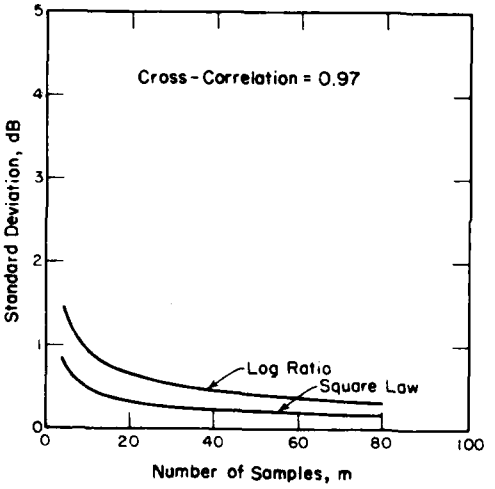

Figure 1b. Standard deviation of estimate of differential reflectivity, expressed in decibels, as a function of the number of samples of each polarization, for a given value of the cross-correlation coefficient, comparing the results due to averaging power, that is, squared amplitude, and the logarithm of power. [After Bringi et al (1983), Reference 8 © IEEE]

3. SIGNAL PROCESSOR DESCRIPTION

In this section we describe the signal processing hardware and the computation of the algorithms discussed in the previous section. Current technology to be incorporated into the new processor makes it possible to reduce the overall size of the processor and increase its computational abilities, in comparison to the present data processor.

Figure 2 is a functional block diagram of the complete system showing the velocity and reflectivity channels. The velocity channel consists of a quadrature

receiver with automatic gain control (AGC), two 8-bit A/D converters, two ground clutter filters, two integrators for averaging the pulse pairs from one and two-pulse time lags, two mean velocity calculators, and a variance calculator using the Srivastava algorithm as described in Section 2.

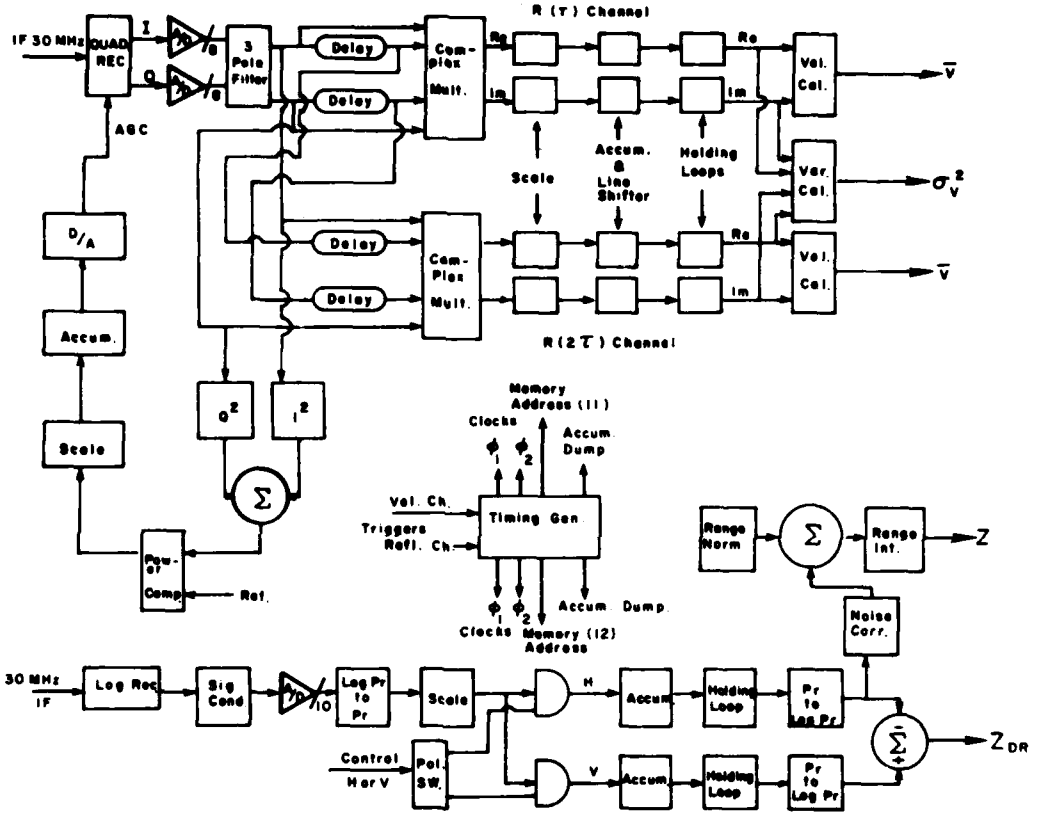

Figure 2. Block diagram of the radar data processor illustrating the calculations of $R(\tau)$, $R(2\tau)$, Z, and Z_{DR}

The reflectivity channel employs a logarithmic receiver, signal conditioner and 10-bit A/D converter, two separate integrator channels for averaging the returns from the two polarizations, namely, horizontal (H) and vertical (V), and a differential reflectivity calculator (Z_{DR}). The horizontal channel is to be used for absolute reflectivity measurements. We added the range correction and range integrator to reduce the number of range cells for archiving and display purposes.

3.1 Autocovariance Calculator

Figure 3 is a more detailed diagram of the autocovariance calculator. For simplicity only the single-lag channel is shown since the two-lag channel is identical. After the signals are filtered to remove ground clutter the inphase and quadrature components are multiplied and summed to form the real and imaginary parts of the autocovariance given by

$$R_n = X_n X_{(n+1)} + Y_n Y_{(n+1)} \tag{31}$$

$$I_n = X_n Y_{(n+1)} - X_{(n+1)} Y_n \tag{32}$$

where X is the inphase component, Y the quadrature, the subscript n denotes the pulse delayed by the interval τ, and $n+1$ denotes the undelayed pulse. The two numbers are then averaged by dividing by the number of pulses integrated (N) and summing them N times in an accumulator as shown in the following equations.

$$\mathrm{Re}[\hat{R}(\tau)] = \sum_{n=1}^{N} \frac{R_n}{N} \tag{33}$$

$$\mathrm{Im}[\hat{R}(\tau)] = \sum_{n=1}^{N} \frac{I_n}{N} . \tag{34}$$

The accumulator is a 2048×25 bit random access memory (RAM). After accumulating over the integration time the memories are then compared range cell by range cell to determine the larger of the two words. The larger word is then shifted in such a manner as to select only the eight most significant bits. The smaller number is shifted an identical amount to keep their ratio the same. The eight bits provide an angular resolution of 0.18° in the argument of the autocovariance. The corresponding velocity resolution is given by

$$\Delta v = (0.18°/180°)\bar{v}_{max} . \tag{35}$$

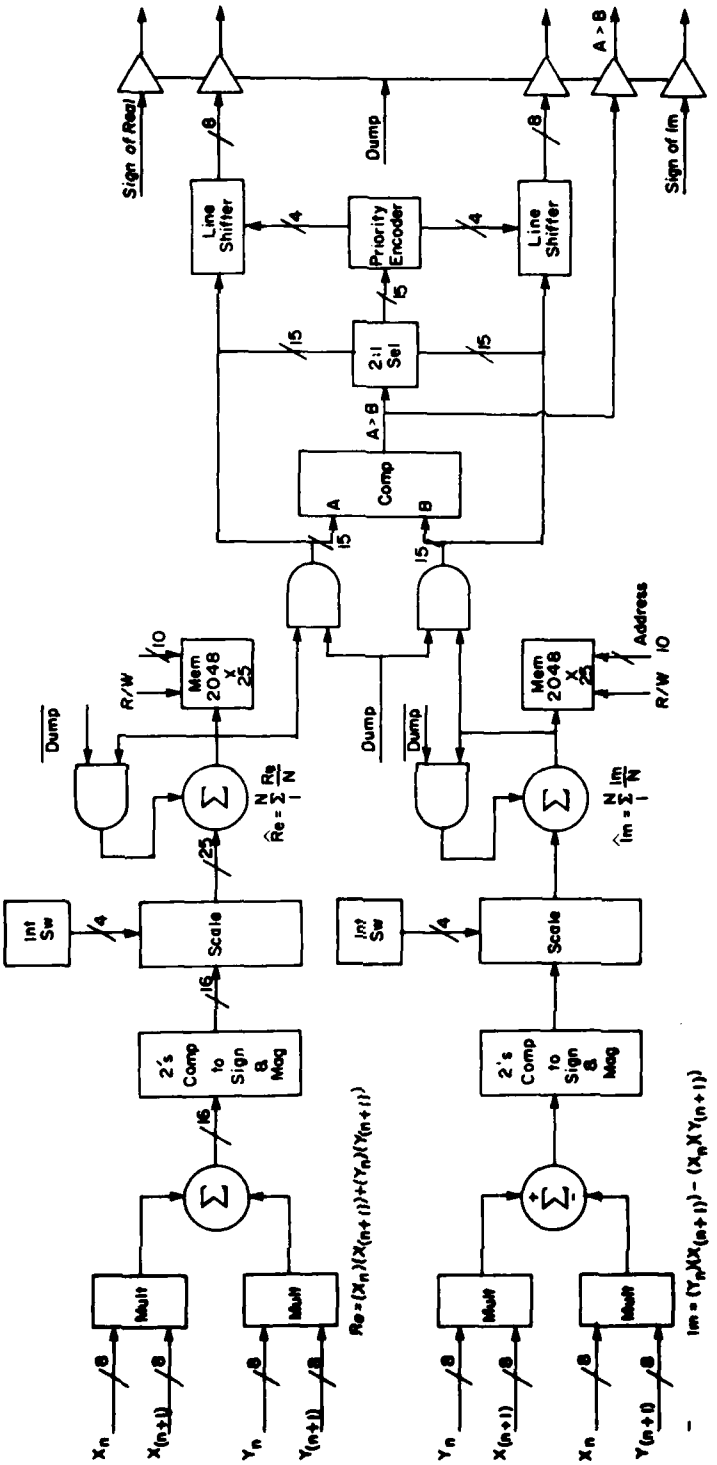

Figure 3. Details of the autocovariance calculator

3.2 Average Velocity Calculator

Figure 4 is a simplified block diagram of the velocity calculator which computes the argument of the autocovariance on a range cell to range cell basis. The real and imaginary numbers from the accumulator are stored in the holding loops and are updated each dump cycle. These holding loops allow for a continuous flow of data words during the accumulating time. In order to perform the calculations in the time alloted we multiply the larger number by the reciprocal of the smaller and take the resultant product to a read only memory (ROM) look up table to obtain the arc tangent. From Figure 4 it can be seen that any argument from 0 to 180° can be calculated unambiguously.

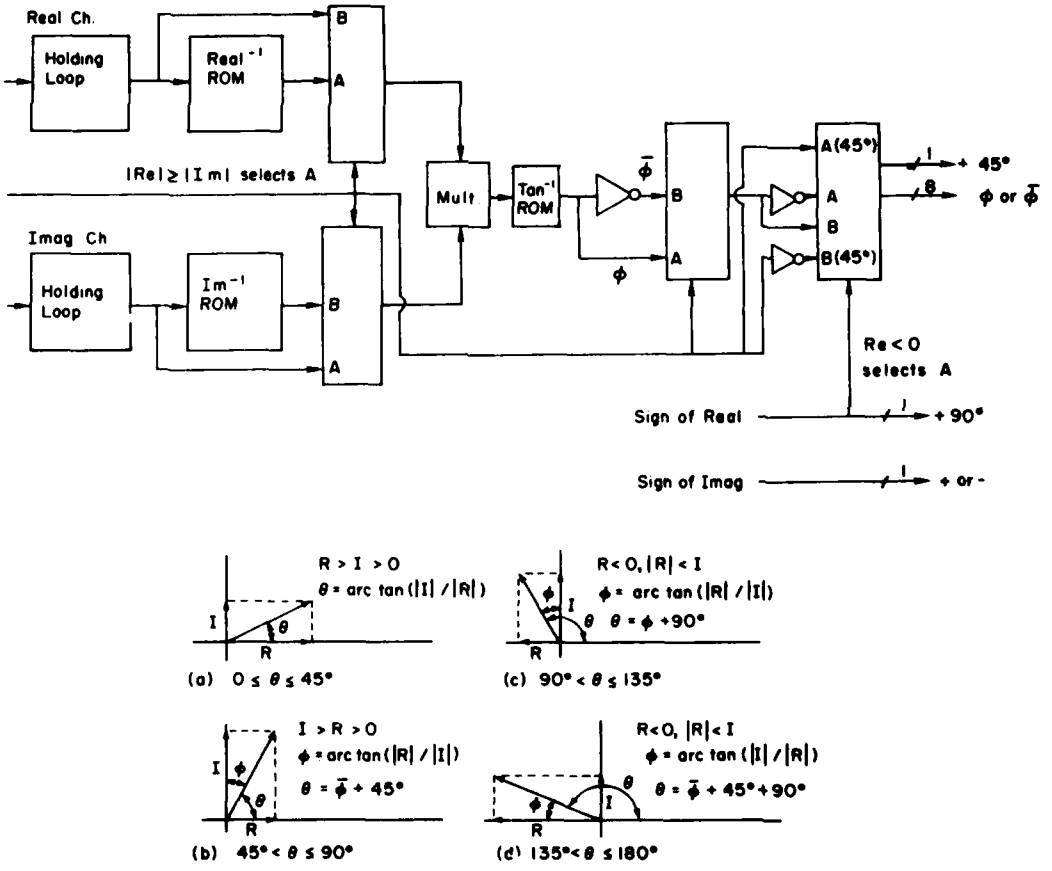

Figure 4. Diagram of mean velocity calculator, illustrating the calculation of the argument angle θ in the domain from 0 to π. The angle ϕ obtained from the arc tangent ROM is between 0° and 45° and is adjusted to yield θ according to the signs and relative magnitudes of the real and imaginary parts of the autocovariance, denoted by R and I. Figures a, b, c, and d illustrate the computations when I > 0; $\bar{\phi}$ is the ones-complement of ϕ and is equal to 45° - ϕ

3.3 Doppler Variance Calculator

The Srivastava algorithm for computing the variance of the Doppler spectrum, given by Eq. (5), requires the absolute value of the autocovariance functions for both the first and second lag pulse pairs, namely $R(\tau)$ and $R(2\tau)$. Since the autocovariance function for each time lag consists of two orthogonal vectors, that is, the real and imaginary parts, we take the square root of the sum of their squares to compute the magnitude of each autocovariance function. Figure 5 is a simplified block diagram of the variance calculator. We perform the high speed division by multiplying the reciprocal of $R(2\tau)$ as obtained from a ROM. The natural logarithm of the resulting quotient, also derived from a ROM, is sent to the display and archiving system. To retain the greatest versatility in the processor we compute the scaling factor, $\frac{\lambda^2}{24\pi^2\tau^2}$, by entering the wavelength (τ) and the pulse repetition time (τ) into the computer that controls the displays and performs other data processing functions.

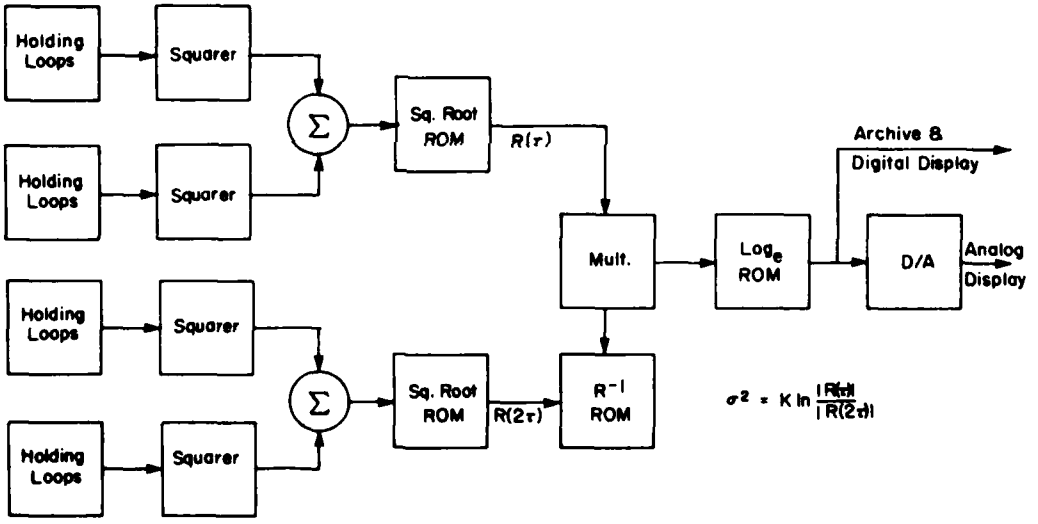

Figure 5. Details of the Doppler variance calculator

3.4 Reflectivity Calculator

Calculation of differential reflectivity, as discussed in Section 2, requires the measurement of the reflectivity factor (Z) at both horizontal and vertical polarizations. The polarization is switched on a pulse-to-pulse basis and the received returns are amplified logarithmically to achieve the dynamic range needed for meteorological signals. The output of the receiver, which is the logarithm of the instantaneous power, is then converted to a 10 bit binary number. A one bit change is approximately equal to a 0.1 dB change in power.

Following the recommendation of Bringi et al[8] we convert the logarithmic output to power by means of a look-up table in the form of a ROM. Floating point notation is used because the range of numbers is far too great to handle by straight binary representation.

Figure 6 is a block diagram of the reflectivity processor. After the conversion to power the returns are separated into two channels, one for horizontal and the other for vertical polarization. An average is calculated in each channel for a number of pulses which is selectable from 2 to 1024 in increments of powers of 2. The averaged returns are then stored in holding loops to provide a continuous output during the averaging time. After the holding loops the average power in each channel is converted back to its logarithm by a ROM. The vertical channel contains a correction factor for calibration differences between the two polarizations, and the differential reflectivity in decibel notation is calculated by taking the difference of the two channels.

The horizontal channel is chosen for computing absolute reflectivity. We correct low signal-to-noise ratios by subtracting from the signal an appropriate number from a look-up table which is based on the ratio of the average signal to average noise. This correction allows for reflectivity values to be calculated down to numbers one bit above average noise. After noise correction, the numbers are corrected for range by adding a correction which is based on the range cell number and obtained from a ROM. Adjacent range cells can be averaged to reduce the number of range samples for archiving purposes and to provide more independent samples in the averages. The output is sent to the archiving and display systems for storage and real time display.

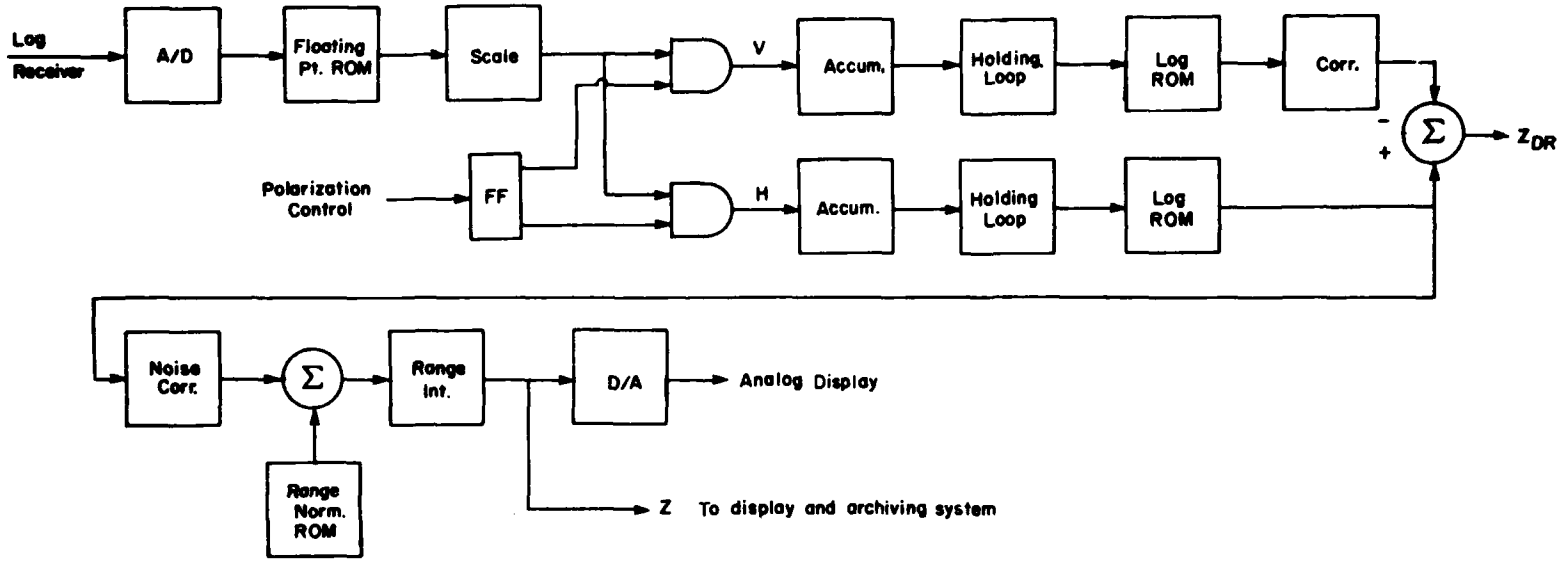

Figure 6. The reflectivity and differential reflectivity calculator

3.5 Timing Generator

Figure 7 shows a simplified block diagram of the timing generator. The reflectivity channel timing generator and the velocity dump generator logic are shown for simplicity. Upon receipt of a reflectivity trigger either a 2 MHz clock from the ground clutter canceller ($\overline{ACX_1}$) or the on-board delay line clock generator is divided to produce either a 1 or 2 μsec pulse train. The delay line clock generator is used when the canceller is not in use. This pulse train is then separated and delayed to produce the various timing clocks needed for memory and processor operation. A modulo 12 memory address counter allows for the storage of the 3066 range cells needed for the 460-km reflectivity coverage. With the use of random access memory in the processor the range cells now span the entire pulse repetition interval regardless of its value.

In order to eliminate pulse pair products involving oppositely polarized pulses, the velocity control logic was devised. Figure 8 shows the timing diagram for this logic for both the one and two lag case with a 4 to 1 ratio of velocity to reflectivity PRF. The shaded area denotes the time for processing. At all other times the output of the complex multiplier is set to zero and its output is not accumulated. Only the processed triggers are counted to determine the integration time of the processor. The number of pulses integrated is accomplished by selecting the proper output for the counter. It is selectable from 2 to 1024 in intervals of powers of 2.

4. OPERATIONAL PROCEDURES AND PARAMETERS

Outputs of the data processor will be displayed and archived by a computer controlled data system. We anticipate that the absolute reflectivity, differential reflectivity, Doppler mean velocity, and Doppler variance will be routinely available for display in plan position or range-height coordinates. Derived parameters such as number concentration and drop size, rainfall rate, wind gradients, and turbulence intensity will be calculated by the computer.

Operational parameters for the radar will include the pulse repetition frequency (PRF) of each of the two transmitters and the polarization switching frequency. It is expected that the polarization will be switched at the PRF of the transmitted signal used for reflectivity measurement and that the PRF of the transmitted signal used for Doppler velocity measurement will be 3 or 4 times higher, as discussed in Section 2. Switch-selectable parameters for the data processor include the number of pulses to be averaged in time and in range for the computation of reflectivity, the number of pulses to be averaged for input to the automatic gain control, and the

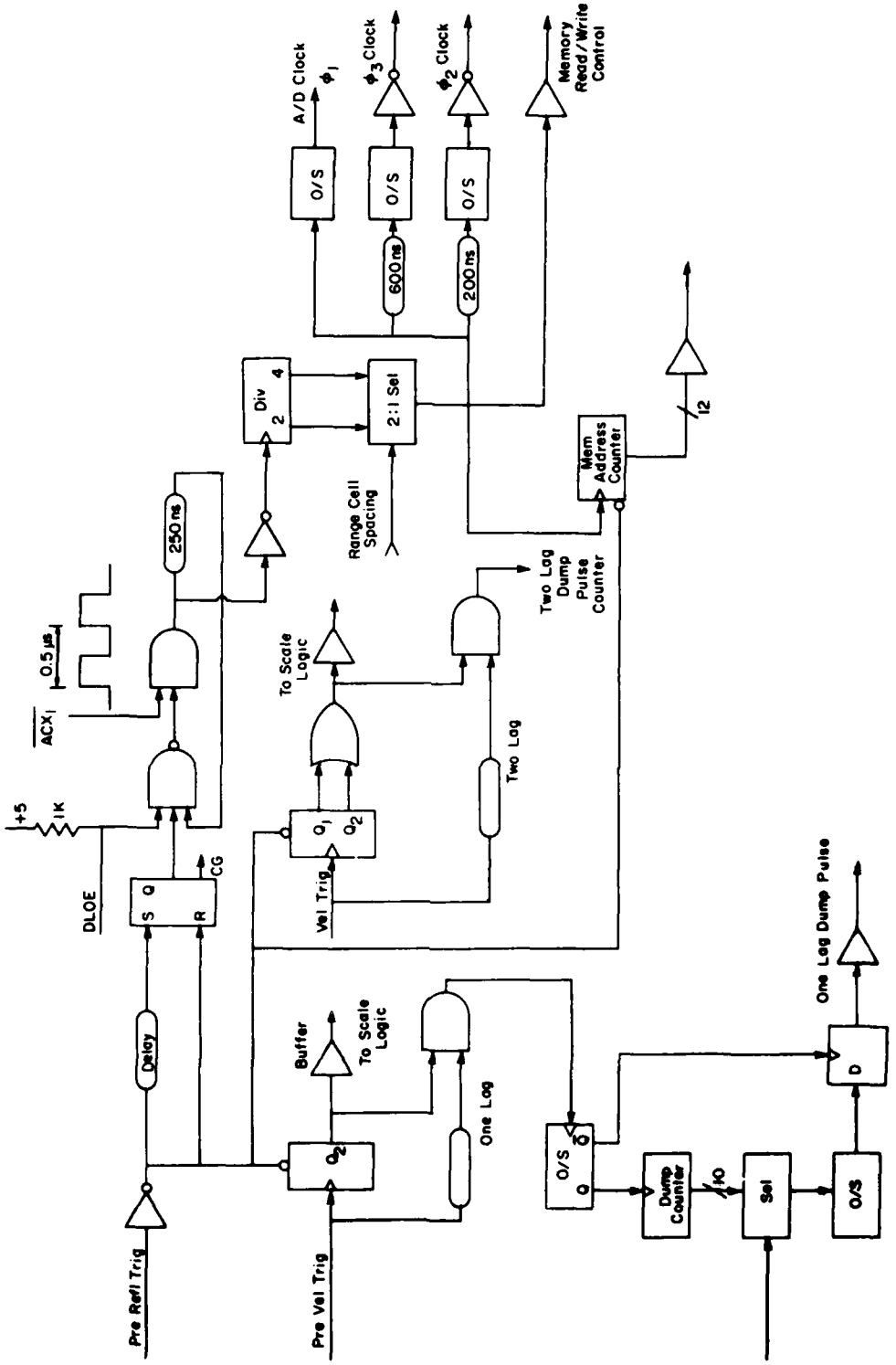

Figure 7. Block diagram of timing generator

number of pulse pairs to be averaged for the autocovariance estimates. The radar wavelength and PRF of the Doppler carrier frequency will be input through the computer for use in scaling the velocity and variance displays, and the peak power of the transmitted signal used for reflectivity measurement will be input for the calculation of reflectivity. All these parameters will be archived, along with the primary data processor outputs and ancillary information such as date, time, and location. The ranges and increments of the control parameters are shown in Table 3.

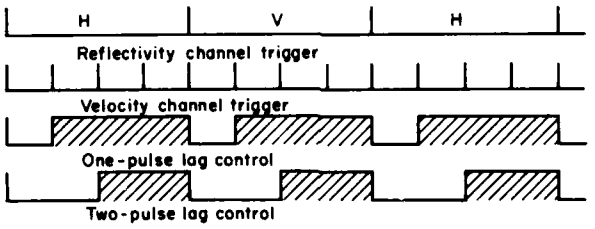

Figure 8. Timing diagram for the computation of differential reflectivity and autocovariance for the case in which the Doppler carrier PRF is four times the reflectivity carrier PRF. The control signals (third and fourth lines) are used to suppress the complex multiplier outputs that correspond to pairs of pulses with opposite polarizations

Table 3. Data Processor Characteristics

Feature	Specification
Range Cells	
Number	Dependent on the pulse repetition time.
Spacing	1 or 2 μsec, selectable
Doppler Channel:	
Integration Type	Rectangular
Pulses Integrated	2^n, n selectable 1 to 10
Range Cells Integrated	Moving average of 2^n, n selectable 0 to 3
Reflectivity Channel:	
Integration Type	Rectangular
Pulses Integrated	2^n, n selectable 1 to 10
Range Cells Integrated	Moving average of 2^n, n selectable 0 to 3
AGC Channel:	
Integration Type	Exponential
Pulses Integrated	2^n, n selectable 0 to 10
Recording:	
Magnetic Tape	Analog, 14 track, serial format
Video Display:	
Type	Real-time, programmable, color

Several procedures may be used to circumvent the problem of range-aliased echoes which may be present in the Doppler channel. Each of these involves a trade-off of sampling time, time resolution of the averaged data, or numerical accuracy. If the PRF of the Doppler carrier frequency is decreased then the increased unambiguous range will encompass all echoes, but the maximum unambiguous Doppler velocity will be decreased. Furthermore, the increased time interval between pluses of the reflectivity carrier frequency will yield a decreased cross-correlation between successive samples of reflectivity at orthogonal polarizations, leading to reduced accuracy of the differential reflectivity. A second procedure is to operate sequentially with fixed and switched polarization, obtaining reflectivity and Doppler velocity measurements from the signals of fixed polarization and obtaining absolute and differential reflectivity from the signals transmitted with alternating polarization. This procedure would necessitate double scanning at low elevation angles and thus increase the time between successive observations of any given region of space. A third alternative is to transmit more than four pulses of the Doppler carrier frequency at each polarization setting. If the returned signal is sampled beginning with the third pulse repetition interval, then aliased echoes of the unwanted polarization will not be present. Although this procedure permits the high unambiguous velocity interval to be maintained, the numerical accuracy of the differential reflectivity will be degraded because of the longer time between the sampling of orthogonal polarizations.

5. CONCLUSIONS

We have developed a design for a data processor capable of computing absolute reflectivity, differential reflectivity, Doppler mean velocity, and Doppler variance from received signals in a radar system transmitting pulses of alternating horizontal and vertical polarization. The velocity parameters are to be derived from estimates of the signal autocovariance function computed by summing the complex products of signal amplitudes at zero, one, and two-pulse time lags. The key design factor here is the need to delete from the summation the products of signals transmitted with different polarization. This need arises from the effects of differential phase shift between the two polarizations in propagation. The reflectivity processor uses floating-point computational hardware to average the received power, rather than its logarithm. This design feature permits the most accurate computation of the differential reflectivity. The processor will be used with a computer-controlled display and archiving system to produce real-time displays of the primary processor outputs and derived meteorological quantities.

References

1. Bishop, A.W., and Armstrong, G.M. (1982) A 10-cm Dual Frequency Doppler Weather Radar, Part I: The Radar System, AFGL-TR-82-0321 (I), AD A125885.

2. Ussailis, J.S., Leiker, L.A., Goodman, R.M., IV, and Metcalf, J.I. (1982) Analysis of a Polarization Diversity Weather Radar Design, AFGL-TR-82-0234, AD A121666.

3. Seliga, T.A., and Bringi, V.N. (1976) Potential use of radar differential reflectivity measurements at orthogonal polarizations for measuring precipitation, J. Appl. Meteor. 15:69-76.

4. Rummler, W.D. (1968) Introduction of a New Estimator for Velocity Spectral Parameters, Tech. Memo. MM-68-4121-5, Bell Telephone Laboratories, Whippany, New Jersey.

5. Strauch, R.G., Kropfli, R.A., Sweezy, W.B., Moninger, W.R., and Lee, R.W. (1978) Improved Doppler velocity estimates by the poly-pulse-pair method. Preprints, 18th Conf. Radar Meteor., Amer. Meteor. Soc., Boston: pp. 376-380.

6. Srivastava, R.C., Jameson, A.R., and Hildebrand, P.H. (1979) Time-domain computation of mean and variance of Doppler spectra. J. Appl. Meteor. 18:189-194.

7. Passarelli, R.E., Jr., and Siggia, A.D. (1983) The autocorrelation function and Doppler spectral moments: Geometric and asymptotic interpretations. J. Clim. Appl. Meteor. 22, accepted for publication

8. Bringi, V.N., Seliga, T.A., and Cherry, S.M. (1983) Statistical properties of the dual-polarization differential reflectivity (Z_{DR}) radar signal. IEEE Trans. Geoscience and Remote Sensing, GE-21:215-220.

END

DATE
FILMED

11-83

DTIC